International Telecommunication Union

ITU-R

Radiocommunication Sector of ITU

Recommendation ITU-R P.682-3
(02/2012)

Propagation data required for the design of Earth-space aeronautical mobile telecommunication systems

P Series
Radiowave propagation

International Telecommunication Union

Foreword

The role of the Radiocommunication Sector is to ensure the rational, equitable, efficient and economical use of the radio-frequency spectrum by all radiocommunication services, including satellite services, and carry out studies without limit of frequency range on the basis of which Recommendations are adopted.

The regulatory and policy functions of the Radiocommunication Sector are performed by World and Regional Radiocommunication Conferences and Radiocommunication Assemblies supported by Study Groups.

Policy on Intellectual Property Right (IPR)

ITU-R policy on IPR is described in the Common Patent Policy for ITU-T/ITU-R/ISO/IEC referenced in Annex 1 of Resolution ITU-R 1. Forms to be used for the submission of patent statements and licensing declarations by patent holders are available from http://www.itu.int/ITU-R/go/patents/en where the Guidelines for Implementation of the Common Patent Policy for ITU-T/ITU-R/ISO/IEC and the ITU-R patent information database can also be found.

Series of ITU-R Recommendations

(Also available online at http://www.itu.int/publ/R-REC/en)

Series	Title
BO	Satellite delivery
BR	Recording for production, archival and play-out; film for television
BS	Broadcasting service (sound)
BT	Broadcasting service (television)
F	Fixed service
M	Mobile, radiodetermination, amateur and related satellite services
P	**Radiowave propagation**
RA	Radio astronomy
RS	Remote sensing systems
S	Fixed-satellite service
SA	Space applications and meteorology
SF	Frequency sharing and coordination between fixed-satellite and fixed service systems
SM	Spectrum management
SNG	Satellite news gathering
TF	Time signals and frequency standards emissions
V	Vocabulary and related subjects

Note: *This ITU-R Recommendation was approved in English under the procedure detailed in Resolution ITU-R 1.*

Electronic Publication
Geneva, 2012

RECOMMENDATION ITU-R P.682-3

Propagation data required for the design of Earth-space aeronautical mobile telecommunication systems

(Question ITU-R 207/3)

(1990-1992-2007-2012)

Scope

This Recommendation describes propagation effects of particular importance to aeronautical mobile-satellite systems. Relevant ionospheric and tropospheric propagation impairments are identified, and reference made to ITU-R Recommendations that provide guidance on these effects. Models are provided to predict the propagation effects caused by signal multipath and scattering from the Earth's surface.

The ITU Radiocommunication Assembly,

considering

a) that for the proper planning of Earth-space aeronautical mobile systems it is necessary to have appropriate propagation data and prediction methods;

b) that the methods of Recommendation ITU-R P.618 are recommended for the planning of Earth-space telecommunication systems;

c) that further development of prediction methods for specific application to aeronautical mobile-satellite systems is required to give adequate accuracy for all operational conditions;

d) that, however, methods are available which yield sufficient accuracy for many applications,

recommends

1 that the methods contained in Annex 1 be adopted for current use in the planning of Earth-space aeronautical mobile telecommunication systems, in addition to the methods recommended in Recommendation ITU-R P.618.

Annex 1

1 Introduction

Propagation effects in the aeronautical mobile-satellite service differ from those in the fixed-satellite service and other mobile-satellite services because:

– small antennas are used on aircraft, and the aircraft body may affect the performance of the antenna;

– high aircraft speeds cause large Doppler spreads;

– aircraft terminals must accommodate a large dynamic range in transmission and reception;

– aircraft safety considerations require a high integrity of communications, making even short-term propagation impairments very important, and communications reliability must be maintained in spite of banking manoeuvres and three-dimensional operations.

This Annex discusses data and models specifically required to characterize the path impairments, which include:

– tropospheric effects, including gaseous attenuation, cloud and rain attenuation, fog attenuation, refraction and scintillation;

– ionospheric effects such as scintillation;

– surface reflection (multipath) effects;

– environmental effects (aircraft motion, sea state, land surface type).

Aeronautical mobile-satellite systems may operate on a worldwide basis, including propagation paths at low elevation angles. Several measurements of multipath parameters over land and sea have been conducted. In some cases, laboratory simulations are used to compare measured data and verify model parameters. The received signal is considered in terms of its possible components: a direct wave subject to atmospheric effects, and a reflected wave, which generally contains mostly a diffuse component.

There is current interest in using frequencies near 1.5 GHz for aeronautical mobile-satellite systems. As most experiments have been conducted in this band, data in this Recommendation are mainly applicable to these frequencies. As aeronautical systems mature, it is anticipated that other frequencies may be used.

2 Tropospheric effects

For the aeronautical services, the altitude of the mobile antenna is an important parameter. Estimates of tropospheric attenuation may be made with the methods in Recommendation ITU-R P.618.

The received signal may be affected both by large-scale refraction and by scintillations induced by atmospheric turbulence. These effects will diminish for aircraft at high altitudes.

3 Ionospheric effects

Ionospheric effects on slant paths are discussed in Recommendation ITU-R P.531. These phenomena are important for many paths at frequencies below about 10 GHz, particularly within ±15° of the geomagnetic equator, and to a lesser extent, within the auroral zones and polar caps. Ionospheric effects peak near the solar sunspot maximum.

Impairments caused by the ionosphere will not diminish for the typical altitudes used by aircraft. A summary description of ionospheric effects of particular interest to mobile-satellite systems is available in Recommendation ITU-R P.680. For most communication signals, the most severe impairment will probably be ionospheric scintillation. Table 1 of Recommendation ITU-R P.680 provides estimates of maximum expected ionospheric effects at frequencies up to 10 GHz for paths at a 30° elevation angle.

4 Fading due to surface reflection and scattering

4.1 General

Multipath fading due to surface reflections for aeronautical mobile-satellite systems differs from fading for other mobile-satellite systems because the speeds and altitudes of aircraft are much greater than those of other mobile platforms.

4.2 Fading due to sea-surface reflections

Characteristics of fading for aeronautical systems can be analysed with procedures similar to those for maritime systems described in Recommendation ITU-R P.680, taking careful account of Earth sphericity, which becomes significant with increasing antenna altitude above the reflecting surface.

4.2.1 Dependence on antenna height and antenna gain

The following simple method, based on a theoretical model, provides approximate estimates of multipath power or fading depth suitable for engineering applications.

The procedure is as follows:

Applicable range:

Frequency: 1-2 GHz

Elevation angle: $\theta_i \geq 3°$ and $G(1.5\theta_i) \geq -10$ dB

where $G(\theta)$ is the main-lobe antenna pattern given by:

$$G(\theta) = -4 \times 10^{-4} \, (10^{G_m/10} - 1) \, \theta^2 \qquad \text{dB} \qquad (1)$$

where:

G_m: value of the maximum antenna gain (dB)

θ: angle measured from boresight (degrees).

Polarization: circular and horizontal polarizations; vertical polarization for $\theta_i \geq 8°$

Sea condition: wave height of 1-3 m (incoherent component fully developed).

Step 1: Calculate the grazing angles of the specular reflection point, θ_{sp}, and the horizon, θ_{hr}, by:

$$\theta_{sp} = 2 \, \gamma_{sp} + \theta_i \qquad \text{degrees} \qquad (2a)$$

$$\theta_{hr} = \cos^{-1} [R_e/(R_e + H_a)] \qquad \text{degrees} \qquad (2b)$$

where:

$\gamma_{sp} =$ $7.2 \times 10^{-3} \, H_a/\tan\theta_i$

R_e: radius of the Earth = 6 371 km

H_a: antenna height (km)

Step 2: Find the relative antenna gain G in the direction midway between the specular point and the horizon. The relative antenna gain is approximated by equation (1) where $\theta = \theta_i + (\theta_{sp} + \theta_{hr})/2$ (degrees).

Step 3: Calculate the Fresnel reflection coefficient of the sea:

$$R_H = \frac{\sin\theta_i - \sqrt{\eta - \cos^2\theta_i}}{\sin\theta_i + \sqrt{\eta - \cos^2\theta_i}} \qquad \text{(horizontal polarization)} \qquad (3a)$$

$$R_V = \frac{\sin\theta_i - \sqrt{(\eta - \cos^2\theta_i)/\eta^2}}{\sin\theta_i + \sqrt{(\eta - \cos^2\theta_i)/\eta^2}} \qquad \text{(vertical polarization)} \qquad (3b)$$

$$R_C = \frac{R_H + R_V}{2} \qquad \text{(circular polarization)} \qquad (3c)$$

$$\eta = \varepsilon_r (f) - j60 \lambda \sigma (f)$$

where:

$\varepsilon_r(f)$: relative permittivity of the surface at frequency f (from Recommendation ITU-R P.527)

$\sigma(f)$: conductivity (S/m) of the surface at frequency f (from Recommendation ITU-R P.527)

λ: free space wavelength (m).

Step 4: Calculate the correction factor C_θ (dB):

$$C_\theta = \begin{cases} 0 & \text{for } \theta_{sp} \geq 7° \\ \theta_{sp} - 7)/2 & \text{for } \theta_{sp} < 7° \end{cases} \quad (4)$$

Step 5: Calculate the divergence factor D (dB) due to the Earth's curvature:

$$D = -10 \log \left[1 + \frac{2 \sin \gamma_{sp}}{\cos \theta_{sp} \sin (\gamma_{sp} + \theta_i)} \right] \quad (5)$$

Step 6: The mean incoherent power of sea reflected waves, relative to the direct wave, P_r, is given by:

$$P_r = G + R + C_\theta + D \qquad \text{dB} \quad (6)$$

where:

$$R = 20 \log \left| R_i \right|$$

with $R_i = R_H$, R_V or R_C from equations (3).

Step 7: Assuming the Nakagami-Rice distribution, fading depth is estimated from:

$$A + 10 \log \left(1 + 10^{P_r/10} \right) \quad (7)$$

where A is the amplitude (dB) read from the ordinate of Fig. 1 of Recommendation ITU-R P.680.

Figure 1 below shows the mean multipath power of the incoherent component obtained by the above method as a function of the elevation angle for different gains. By comparing with the case of maritime mobile-satellite systems (Fig. 2 of Recommendation ITU-R P.680), it can be seen that the reflected wave power P_r for aeronautical mobile-satellite systems is reduced by 1 to 3 dB at low elevation angles.

FIGURE 1

Mean multipath power relative to direct signal power as a function of elevation angle for different antenna gains

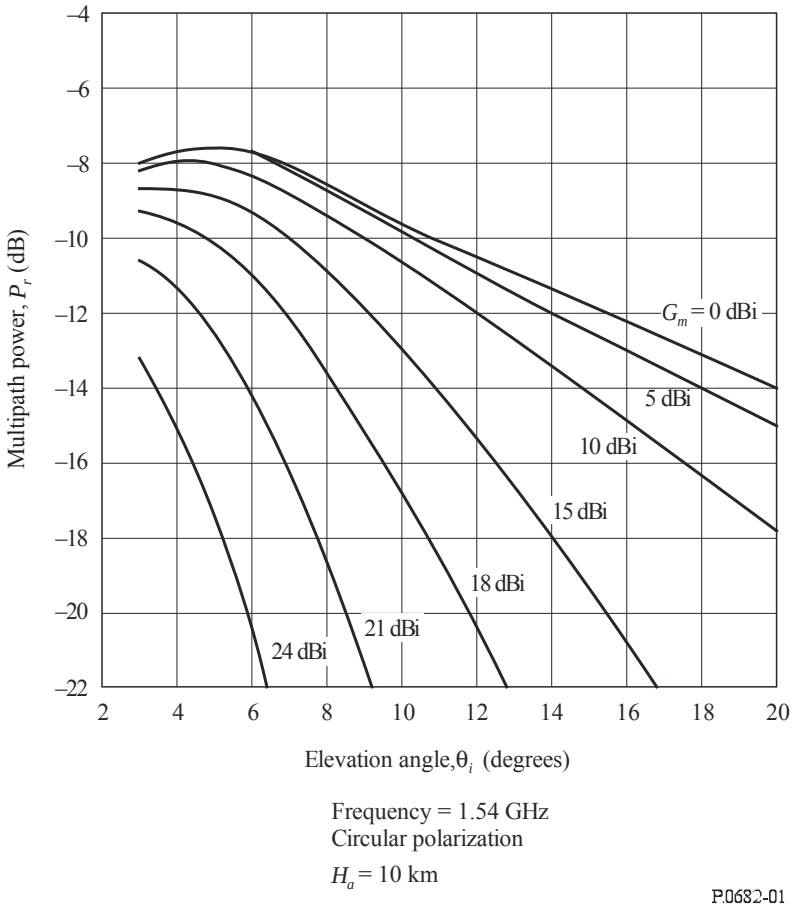

NOTE 1 – Analytical as well as experimental studies have shown that for circularly polarized waveforms at or near 1.5 GHz and an antenna gain of 7 dB, multipath fade depth for rough sea conditions is about 8 to 11 dB for low and moderate aircraft heights and about 7 to 9 dB for high altitudes (above 2 km). Multipath fade depth is about 2 dB lower for a 15 dB antenna gain.

4.2.2 Delay time and correlation bandwidth

The received signal consists of the direct and the reflected waveforms. Because the reflected component experiences a larger propagation delay than the direct component, the composite received signal may be subject to frequency-selective fading. Signal correlation decreases with increasing frequency separation. The dependence of correlation on the antenna gain is small for gains below 15 dB. Figure 2 shows the relationship between antenna height and the correlation bandwidth, defined here as the frequency separation for which the correlation coefficient between two radio waves equals 0.37 ($1/e$). The correlation bandwidth decreases as the antenna altitude increases, becoming about 10 to 20 kHz (delay time of 6 to 12 μs) for an antenna at an altitude of 10 km. Thus, multipath fading for aeronautical systems may have frequency-selective characteristics.

FIGURE 2

Correlation bandwidth vs antenna altitude for antenna gain of 10 dBi

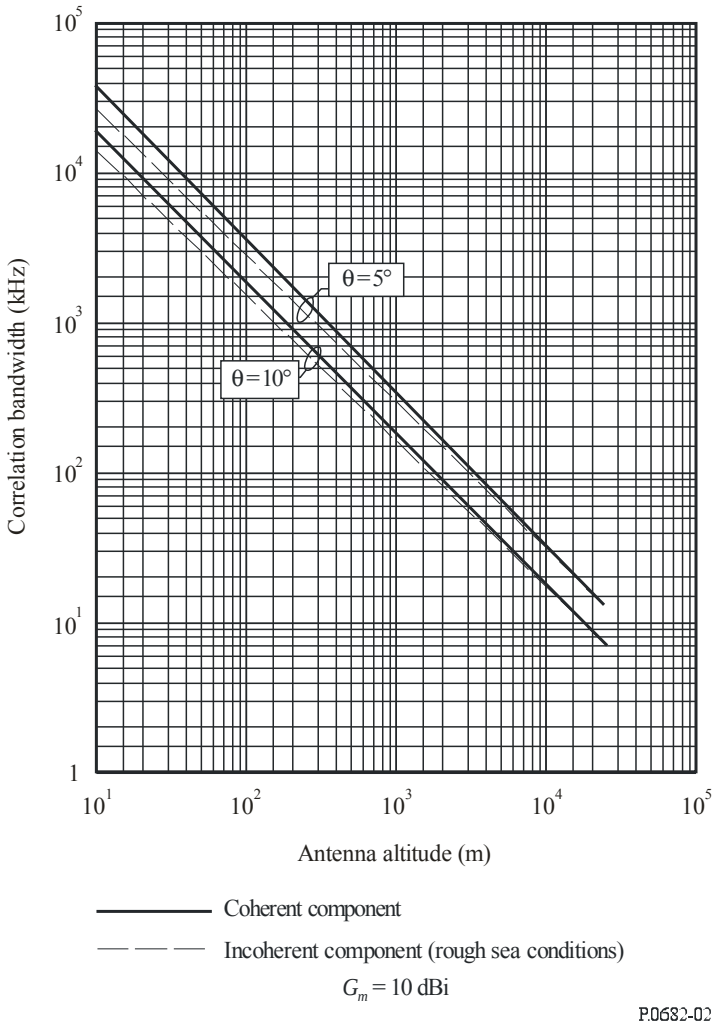

4.3 Measurements of sea-reflection multipath effects

Extensive experiments have been conducted in the 1.5 to 1.6 GHz band. Results of these measurements are summarized in this section for application to systems design.

Table 1 summarizes the oceanic multipath parameters observed in measurements, augmented with results from an analytical model. The delay spreads in Table 1 are the widths of the power-delay profile of the diffusely-scattered signal arriving at the receiver. The correlation bandwidth given in Table 1 is the 3 dB bandwidth of the frequency autocorrelation function (Fourier transform of the delay spectrum). Doppler spread is determined from the width of the Doppler power spectral density. The decorrelation time is the 3 dB width of the time autocorrelation function (inverse Fourier transform of the Doppler spectrum).

TABLE 1

Multipath parameters from ocean measurements

Parameter	Measured range	Typical value at specified elevation angle		
		8°	**15°**	**30°**
Normalized multipath power (dB)				
Horizontal polarization	–5.5 to –0.5	–2.5	–1	–1
Vertical polarization	–15 to –2.5	–14	–9	–3.5
Delay spread[1] (μs)				
3 dB value	0.25-1.8	0.6	0.8	0.8
10 dB value	2.2 -5.6	2.8	3.2	3.2
Correlation bandwidth[2]				
3 dB value (kHz)	70-380	160	200	200
Doppler spread[1] (Hz)				
In-plane geometry				
3 dB value	4-190	5	70	140
10 dB value	13-350	44 40[3]	180	350
Cross-plane geometry				
3 dB value	79-240	79	110	190
10 dB value	180-560	180 80[3]	280	470
Decorrelation time[2] (ms)				
3 dB value	1.3-10	7.5	3.2	2.2

[1] Two-sided.

[2] One-sided.

[3] Data from multipath model for aircraft altitude of 10 km and aircraft speed of 1 000 km/h.

Normalized multipath power for horizontal and vertical antenna polarizations for calm and rough sea conditions are plotted versus elevation angle in Fig. 3, along with predictions derived from a physical optics model. Sea condition has a minor effect for elevation angles above about 10°. The agreement between measured coefficients and those predicted for a smooth flat Earth as modified by the spherical-Earth divergence factor increases as sea conditions become calm.

FIGURE 3

Oceanic normalized multipath power vs elevation angle at 1.6 GHz

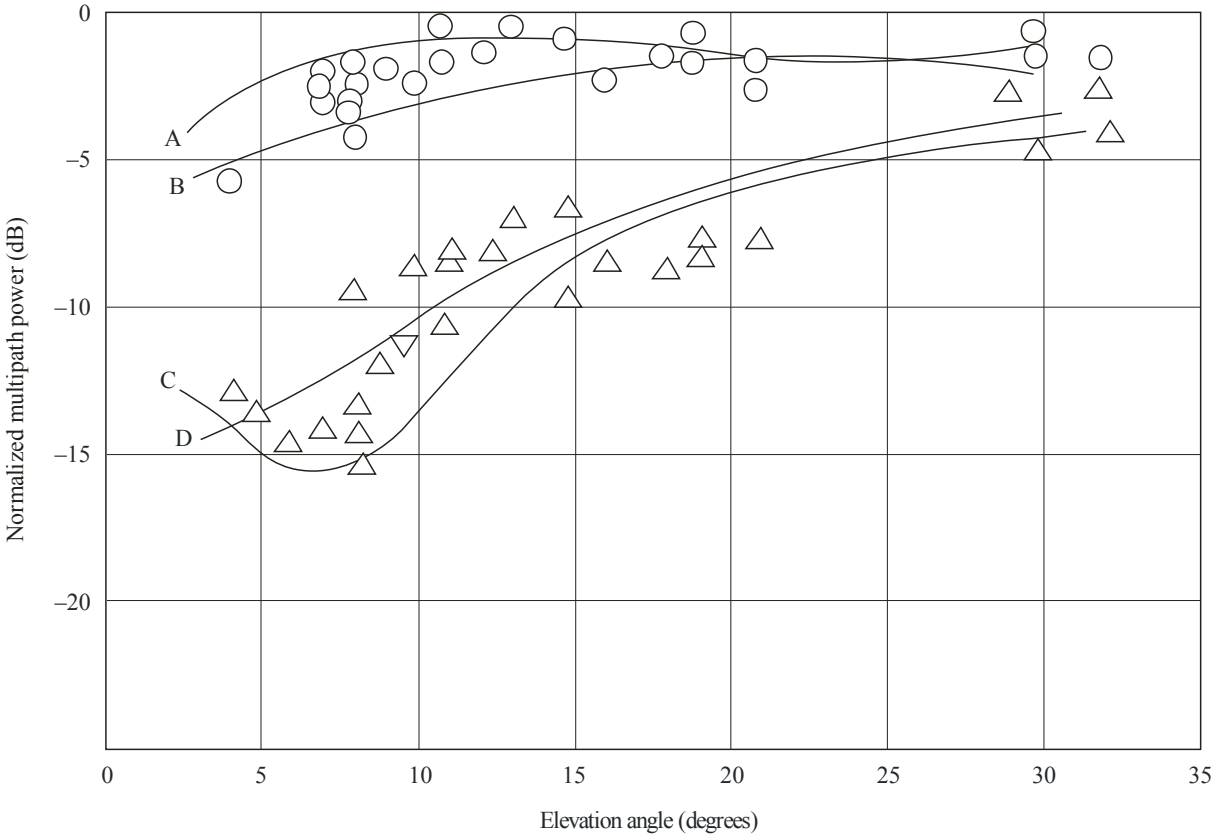

O : horizontal polarization measurements
Δ : vertical polarization measurements

Curves A : horizontal polarization prediction, calm sea
B : horizontal polarization prediction, rough sea
C : vertical polarization prediction, calm sea
D : vertical polarization prediction, rough sea

P.0682-03

Multipath data were collected in a series of aeronautical mobile-satellite measurements conducted over the Atlantic Ocean and parts of Europe. Figure 4 shows the measured mean and standard deviations of 1.6 GHz fade durations as a function of elevation angle for these flights. (A crossed-dipole antenna with a gain of 3.5 dBi was used to collect these data. The aircraft flew at a nominal altitude of 10 km and with a nominal ground speed of 700 km/h.).

FIGURE 4

Fade duration vs elevation angle for circular polarization at 1.6 GHz (antenna gain = 3.5 dBi); data collected over Atlantic Ocean and W. Europe

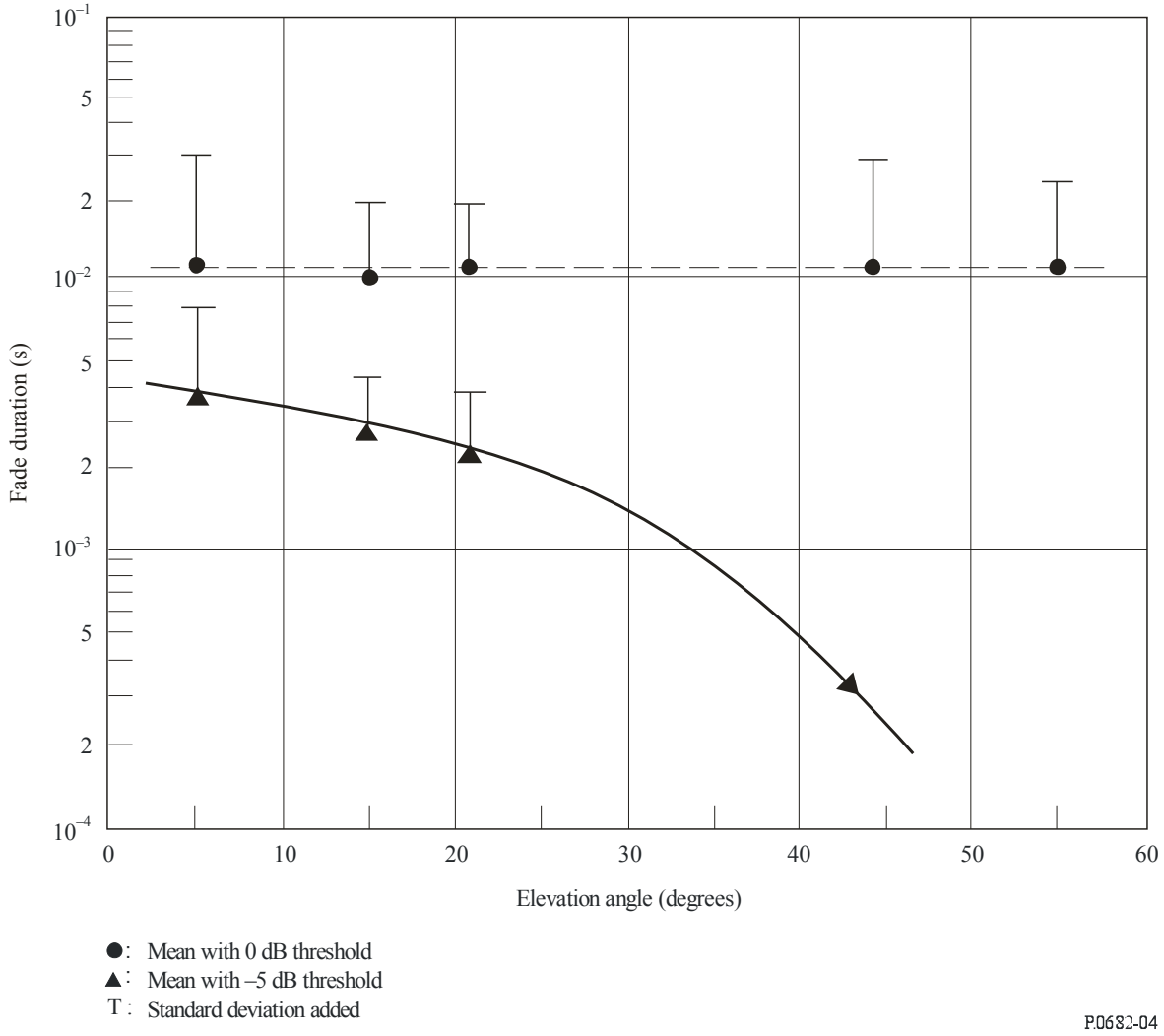

4.4 Measurements of land-reflection multipath effects

Table 2 supplies multipath parameters measured during flights over land; parameter definitions are the same as for Table 1. Land multipath signals are highly variable. No consistent dependence on elevation angle has been established, perhaps because ground terrain is highly variable (data were collected over wet and dry soil, marshes, dry and wet snow, ice, lakes, etc.).

NOTE 1 – Irreducible error rate; multipath fading in mobile channels gives rise to an irreducible error rate at which increases in the direct signal power do not reduce the corresponding error rate. Simulations indicate that the irreducible error rate is higher for an aeronautical mobile-satellite channel than for a land mobile-satellite channel.

TABLE 2

Multipath parameters from land measurements

Parameter	Measured range	Typical value
Normalized multipath power (dB)		
Horizontal polarization	–18 to 2	–9
Vertical polarization	–21 to –3	–13
Delay spread[1] (μs)		
3 dB value	0.1-1.2	0.3
10 dB value	0.2-3	1.2
Correlation bandwidth[2] (kHz)		
3 dB value	150-3 000	600
Doppler spread[1] (Hz)		
3 dB value	20-140	60
10 dB value	40-500	200
Decorrelation time[2] (ms)		
3 dB value	1-10	4

[1] Two-sided.

[2] One-sided.

4.5 Multipath model for aircraft during approach over land and during landing

Short-delayed multipath in aeronautical communication and navigation systems has to be considered especially for broadband signals. The reflections on the aircraft structure produce significant disturbances. Especially during the final approach when communication availability and reliability as well as navigation accuracy and integrity are most important, the ground reflection and the reflection on the fuselage generate significant propagation effects.

Although the model primarily targets navigation applications, it is of course possible to use it with any satellite signal. However, due to the primary expected usage, the antenna is assumed to be on top of the cockpit (where usually a navigation antenna is placed). The complete model is intended to be used as a statistical simulator. Since the bandwidths of the reflections appear to be very low, the process will not yield sufficient statistics during the approach time of 200 s. To simulate a statistically valid navigation error, the model must be used for a large number of approaches. The simulation results of these approaches must be averaged to obtain the minimum, maximum and average navigation error.

A software implementation of the model is available on that part of the ITU-R website related to Radiocommunication Study Group 3.

4.5.1 Physical effects

The multipath propagation conditions of a receiving aircraft divide in two main parts:

– the aircraft structure; and

– the ground reflection.

The aircraft structure shows significant reflections only on the fuselage (when the antenna is mounted at the top of the cockpit). This very short-delayed reflection shows little time variance and dominates the channel.

A strong wing reflection was not observed (when the antenna is mounted at the top of the cockpit).

The ground reflection shows high time variance and is Doppler-shifted according to the aircraft sink rate.

4.5.2 Valid range of model

The model can be used for frequencies between 1 GHz and 3 GHz. The satellite azimuth can vary between 10° and 170°, or 190° and 350°. The elevation angle to the satellite can vary between 10° and 75°.

4.5.3 Model

4.5.3.1 Overview

FIGURE 5

Complete aeronautical channel model

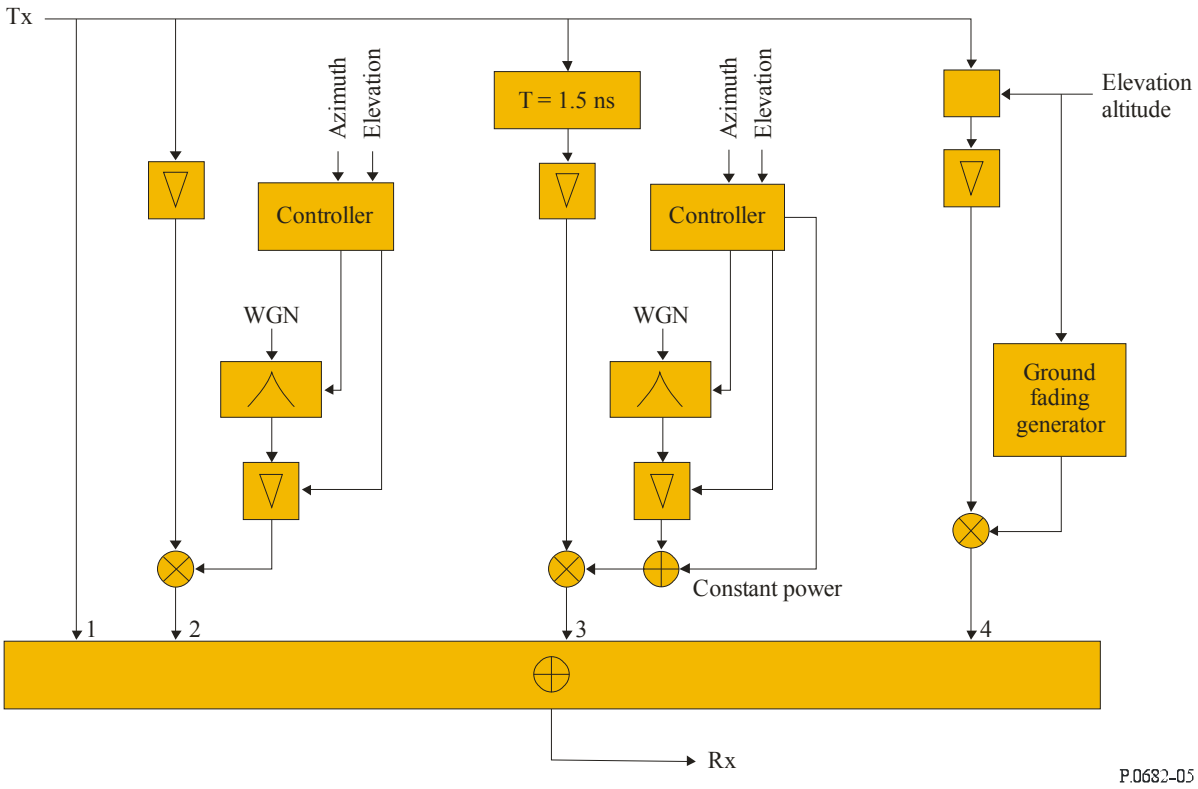

Figure 5 shows the complete aeronautical model for the final approach. The first branch is the direct signal (Branch 1), followed by the flat fading part modelling the line-of-sight (LoS) modulation (Branch 2). The third branch (Branch 3) consists of the fuselage multipath fading process, which is delayed by 1.5 ns. The last branch (Branch 4) is the ground echo, whose delay depends on elevation and altitude.

Time-variant input parameters of this model are:

– satellite azimuth, $\varphi(t)$

– satellite elevation, $\theta(t)$

– altitude of the aircraft (above ground), $h(t)$, where t denotes the time.

In addition the model requires the knowledge of the aircraft geometry and flight dynamics. Empirical coefficients are presented for the following aircraft types:

– Vereinigte Flugzeugwerke VFW 614 (ATTAS), representing a small jet

– Airbus A 340, representing a large commercial jet.

The azimuth and elevation dependence of the multipath fading processes, which are indicated in the above diagram as "controller", are taken into account by the polynomial function used in equation (10). Furthermore, the delay of the ground reflection is a function of elevation and altitude; see equation (16).

The fading processes and time-variant blocks have input parameters for adjusting the model to different satellite positions (elevation and azimuth). The various fading processes are strongly dependent on the aircraft type.

TABLE 3

The parameters of the channel model – Overview

	Delay (ns)	**Relative power (dB)**	**Doppler bandwidth (Hz)**
LoS DC component Fading process	0	0 (–14.2 – *mean*)	0 < 0.1
Fuselage DC component Fading process	1.5	–14.2 (–14.2 – *mean*)	 < 0.1
Ground	900-10 (descending)	–15 to –25	< 20 (biased due to sink rate)

4.5.3.2 Direct path

Beside the LoS (Branch 1), this path is affected by a strong modulation (Branch 2), which has a Rician amplitude distribution. This fading process is generated as given in equations (8), (9), (10) and (11).

4.5.3.3 Wing reflection

If the antenna is placed on the top of the cockpit (which is mandatory for satellite navigation antennas), the incoming ray is dispersed over a large angular range. Therefore the total power of the wing reflection is negligible (below –35 dB).

For antennas located at other positions (e.g. for communication systems), especially between the wings, a wing reflection contribution might be expected.

4.5.3.4 Fuselage reflection

To generate a time series of the fuselage reflection, the knowledge of its power spectral density is essential. The model is driven by a stochastic process, p_{proc}. This process can be generated by filtering complex white noise with the power spectral density given in equation (8), where b_2 and b_3 are the coefficients of the exponential process:

$$p_{proc}(\text{dB}) = b_1 + b_2 \cdot \text{e}^{b_3 \cdot |f|} \tag{8}$$

In addition to this noisy process, the fuselage reflection signal contains a mean (DC) component of −14.2 dB and the constant b_1 has been determined as:

$$b_1 = -14.2 - mean \qquad \text{(dB)} \tag{9}$$

As noted previously, the valid path elevation angle range is between 10° and 75°. The azimuth can vary from 15° to 165° and 195° to 335°, respectively.

To derive the *mean* and b_2 and b_3 coefficients, a 2-dimensional polynomial function of 4th order to each parameter (mean, b_2, b_3) is given. As an example,

$$mean(\theta, \varphi) = \left[\theta^4 \;\; \theta^3 \;\; \theta^2 \;\; \theta \;\; 1\right] \cdot A_{mean} \cdot \begin{bmatrix} \varphi^4 \\ \varphi^3 \\ \varphi^2 \\ \varphi \\ 1 \end{bmatrix} \tag{10}$$

gives the mean value as a function of elevation θ and azimuth φ, where A_{mean} is a 5-by-5 matrix of polynomial coefficients. Coefficients b_2 and b_3 are calculated similarly.

For the two aircraft examples (ATTAS and A340), these matrices are given respectively by:

$A_{mean,ATTAS} =$

$$\begin{bmatrix} -2.0057e-12 & 5.0499e-10 & -4.6114e-8 & 1.8053e-6 & -2.4773e-5 \\ 2.8598e-10 & -7.4259e-8 & 7.0553e-6 & -2.9116e-4 & 0.0043 \\ -1.1568e-8 & 3.2474e-6 & -3.3846e-4 & 0.0156 & -0.2698 \\ 3.8681e-8 & -2.2536e-5 & 0.0038 & -0.2512 & 6.3140 \\ 1.9434e-6 & -3.5747e-4 & 0.0133 & 0.8133 & -28.1329 \end{bmatrix}$$

$A_{b3,ATTAS} =$

$$\begin{bmatrix} -1.8398e-12 & 4.2182e-10 & -3.3813e-8 & 1.0855e-6 & -1.0875e-5 \\ 2.6665e-10 & -6.0897e-8 & 4.8490e-8 & -1.5346e-4 & 0.0015 \\ -1.2870e-8 & 2.2917e-6 & -2.2947e-4 & 0.0071 & -0.0629 \\ 2.3542e-7 & -5.2520e-5 & 0.0040 & -0.1193 & 0.9153 \\ 1.2058e-6 & 2.5797e-4 & -0.0187 & 0.5027 & -4.1128 \end{bmatrix}$$

$A_{b2,ATTAS} =$

$$\begin{bmatrix} -3.9148e-11 & 8.8672e-9 & -7.0048e-7 & 2.2069e-5 & -2.1492e-4 \\ 6.0699e-9 & -1.3708e-6 & 1.0784e-4 & -0.0034 & 0.0322 \\ -3.2203e-7 & 7.2344e-5 & -0.0057 & 0.1747 & -1.6206 \\ 6.7649e-6 & -0.0015 & 0.1162 & -3.5328 & 31.6814 \\ -4.4741e-5 & 0.0098 & -0.7383 & 21.9981 & -142.3524 \end{bmatrix} \tag{11}$$

$$A_{means,A340} =$$
$$\begin{bmatrix} -2.6220e-12 & 6.0886e-10 & -5.0686e-8 & 1.8074e-6 & -2.3633e-5 \\ 4.3848e-10 & -1.0231e-7 & 8.6113e-6 & -3.1465e-4 & 0.0044 \\ -2.3577e-8 & 5.5538e-6 & -4.7815e-4 & 0.0184 & -0.2872 \\ 3.9552e-7 & -9.2657e-5 & 0.0082 & -0.3431 & 6.9937 \\ -1.5225e-6 & 3.3690e-4 & -0.0312 & 1.7110 & -32.8066 \end{bmatrix}$$

$$A_{b3,A340} =$$
$$\begin{bmatrix} -1.2021e-12 & 2.7780e-10 & -2.2626e-8 & 7.4413e-7 & -7.5120e-6 \\ 1.7647e-10 & -4.0725e-8 & 3.3131e-6 & -1.0855e-4 & 0.0011 \\ -8.6470e-9 & 1.9871e-6 & -1.6099e-4 & 0.0052 & -0.0488 \\ 1.6123e-7 & -3.6656e-5 & 0.0029 & -0.0946 & 0.8204 \\ -8.5647e-7 & 1.8942e-4 & -0.0149 & 0.4826 & -5.5011 \end{bmatrix}$$

$$A_{b2,A340} =$$
$$\begin{bmatrix} -3.1880e-11 & 7.2724e-9 & -5.8454e-7 & 1.9069e-5 & -1.9707e-4 \\ 4.7229e-9 & -1.0775e-6 & 8.6761e-5 & -0.0028 & 0.0293 \\ -2.3471e-7 & 5.3437e-5 & -0.0043 & 0.1413 & -1.4541 \\ 4.4756e-6 & -0.0010 & 0.0812 & -2.6731 & 27.5448 \\ -2.5361e-5 & 0.0056 & -0.4459 & 14.8917 & -109.1083 \end{bmatrix}$$

4.5.3.5 Ground reflection

The ground reflection is Doppler-shifted by the aircraft sink rate (vertical speed), $v_{vert}(t)$. Its Doppler offset is given by:

$$f_{ground}(t) = \frac{v_{vert}(t)}{\lambda} \tag{12}$$

where λ denotes the wavelength. Around the mean frequency, given in equation (12), the Doppler spectrum of the ground reflection is well represented by the normalized Gaussian distribution:

$$P_{Gr(\mathrm{dB})} = P_{g(\mathrm{dB})} + 20\log_{10}\left(\frac{1}{\sigma\sqrt{2\pi}} \cdot \mathrm{e}^{-\frac{f^2}{2\sigma^2}}\right) \tag{13}$$

P_g denotes the power of the ground reflection obtained by the Markov model, where the standard deviation has been found experimentally to be:

$$\sigma = 2.92 \text{ Hz} \tag{14}$$

To model the ground reflection, the final approach is divided into three different zones of altitude (high, mid and low altitude). In each zone, the ground reflection is characterized by a Markov state model.

TABLE 4

Altitude regions for the Markov model

Level	From (m)	To (m)
"High"	1 000	400
"Mid"	400	100
"Low"	100	10

FIGURE 6

Altitude regions of the ground model

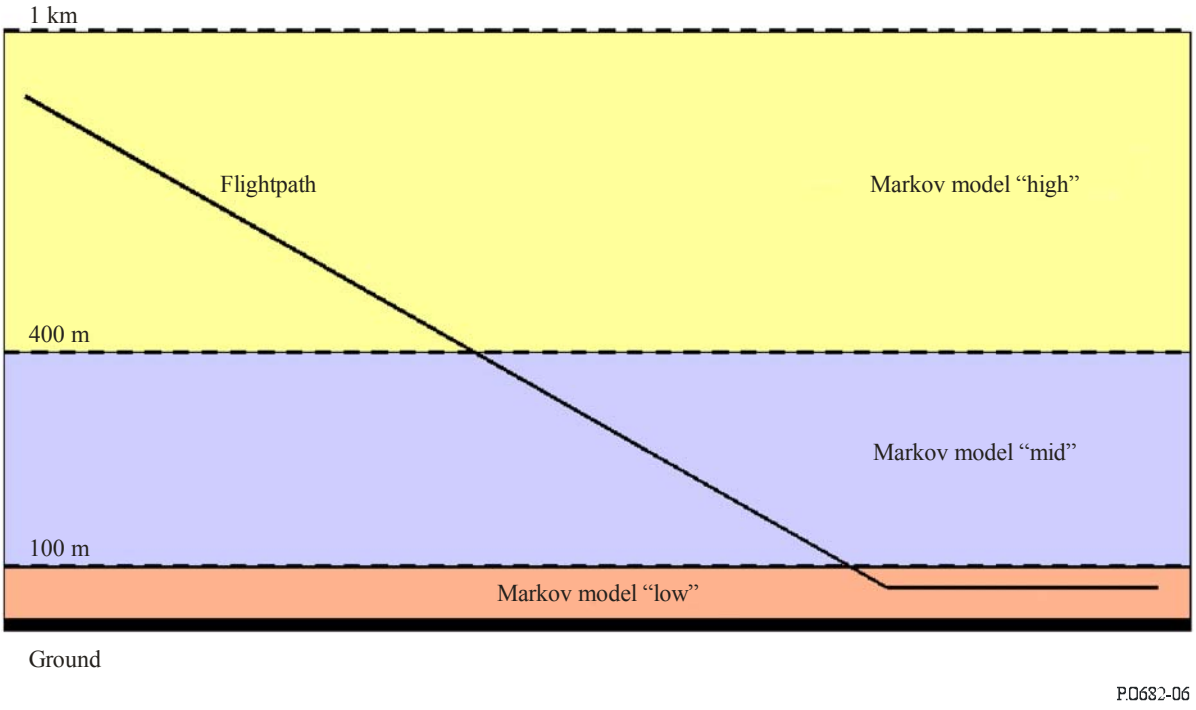

TABLE 5

States of the ground fading Markov model

State	Power (dB)
1[(1)]	< –25
2	–23
3	–19
4	–15

(1) No ground reflection.

FIGURE 7

Realisation of the ground fading generator module

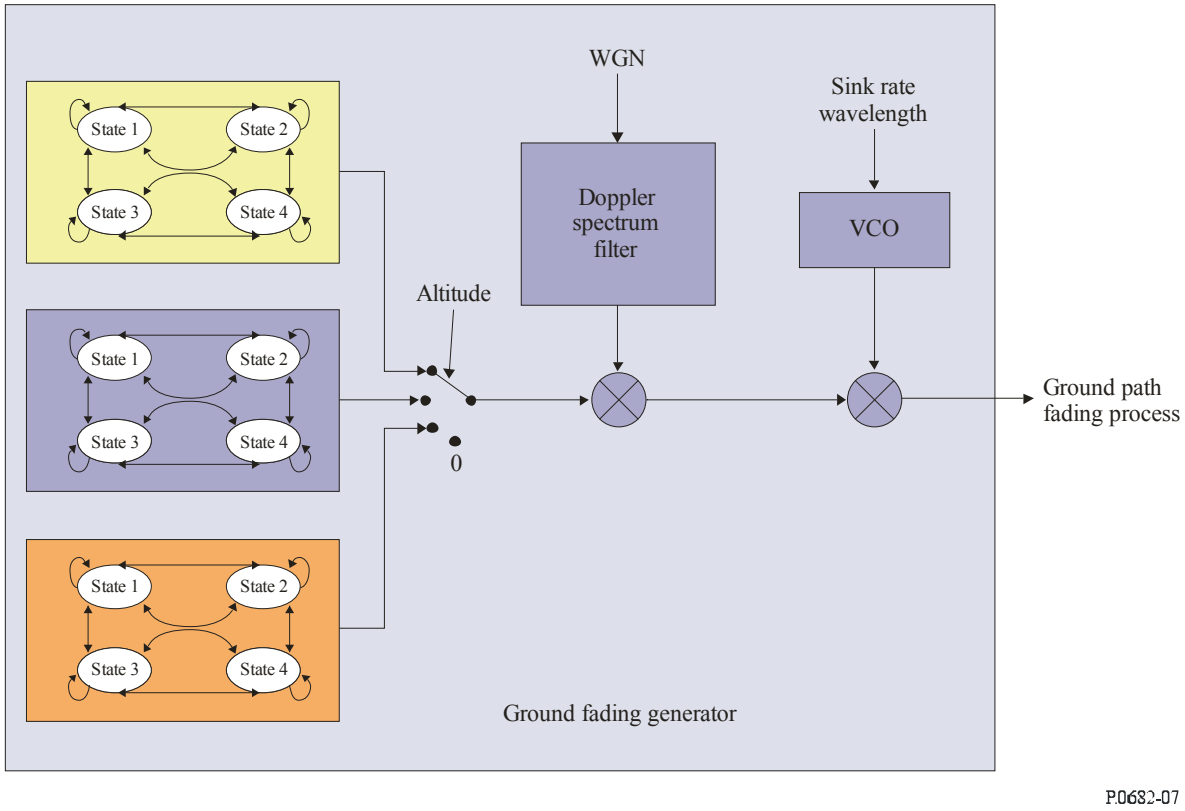

The Markov transition probabilities are obtained from the quantised measurement data. The transition matrix P, where $P_{x,y}$ is the probability of changing from state x to state y, is determined for each altitude region independently.

The ground fading process is generated by an altitude-dependent Markov model for a sampling frequency of 25.4 Hz. Note that these transition probabilities are only valid for this frequency. The transition altitudes are given by Table 4 and illustrated in Fig. 6.

The output power states of the model are depicted in Table 5 and illustrated in Fig. 7.

From the measurements the following transition probability matrices were derived,

$$P_{400-1000} = \begin{bmatrix} 0.9866 & 0.0087 & 0.0047 & 0 \\ 0.6087 & 0.3043 & 0.0870 & 0 \\ 0.2143 & 0.3571 & 0.4286 & 0 \\ 0.3333 & 0.3333 & 0.3334 & 0 \end{bmatrix}$$

$$P_{100-400} = \begin{bmatrix} 0.9842 & 0.0130 & 0.0028 & 0 \\ 0.6667 & 0.2222 & 0.0889 & 0.0222 \\ 0.0667 & 0.1167 & 0.5000 & 0.3166 \\ 0 & 0 & 0.3279 & 0.6721 \end{bmatrix} \quad (15)$$

$$P_{10-100} = \begin{bmatrix} 0.9645 & 0.0310 & 0.0045 & 0 \\ 0.7308 & 0.1538 & 0.1154 & 0 \\ 0.6250 & 0.1250 & 0.2500 & 0 \\ 0.3333 & 0.3333 & 0.3334 & 0 \end{bmatrix}$$

$$P_{0-10} = \begin{bmatrix} 1 & 0 & 0 & 0 \\ 1 & 0 & 0 & 0 \\ 1 & 0 & 0 & 0 \\ 1 & 0 & 0 & 0 \end{bmatrix}$$

where P_{x-y} denotes the transition probability in the altitude region $h(t) \geq x$ and $h(t) < y$.

Note that this Markov model describes a landing in Graz airport in Austria. This region is dominated by forests, grasslands and occasionally streets. Weather conditions, environment, flight geometry and many other parameters may influence on the characteristics of the ground echo. So these numbers are to be seen as parameters to be adapted by the user if intended for other region types. In particular, an approach over (salt) water or a region with many canals is expected to show rather different behaviour.

The delay of the ground reflection as a function of the path elevation angle can be easily calculated assuming a flat environment around the airport by

$$\tau_{ground}(t) = \frac{2 \cdot h(t) \cdot \sin(\theta)}{c} \quad (16)$$

where:

c: speed of light

$h(t)$: aircraft altitude

θ: elevation angle.